Acute Loss of Adipose Tissue-Derived Adiponectin Triggers Immediate Metabolic Deterioration

Jonathan Y. Xia[1], Kai Sun[1,2], Chelsea Hepler[1], Alexandra L. Ghaben[1], Rana K. Gupta[1], Yu A. An[1], William L. Holland[1], Thomas S. Morley[1], Andrew C. Adams[3], Ruth Gordillo[1], Christine M. Kusminski[1] and Philipp E. Scherer[1,4]

[1]Touchstone Diabetes Center, Department of Internal Medicine, The University of Texas Southwestern Medical Center, Dallas, Texas, USA, 75390-8549
[2] Center for Metabolic and Degenerative Diseases, Institute of Molecular Medicine, University of Texas Health Science Center at Houston. Houston, TX, USA, 77030
[3]Lilly Research Laboratories, Division of Eli Lilly and Company, Indianapolis, Indiana, USA
[4]Department of Cell Biology, The University of Texas Southwestern Medical Center, Dallas, Texas, USA, 75390-8549

Correspondence should be addressed to: P.E.S.
Touchstone Diabetes Center, UT Southwestern Medical Center, 5323 Harry Hines Blvd, MC8549, Dallas, TX 75390-8549
e-mail: philipp.scherer@UTSouthwestern.edu

ESM Methods

Generation of floxed adiponectin locus

To generate the *Adiponectin* floxed mice, genomic regions of the mouse *Adiponectin* locus were isolated from 129SvEv genomic DNA by high-fidelity PCR (Roche Expand Long Template PCR System or Roche High Fidelity PCR System) and cloned into pGKF2L2DT [1]. A 5.0-kb genomic sequence (5' targeting arm, long arm) upstream of *Adiponectin* exon 2, bounded by an upstream SacII site and a downstream NotI site, was cloned upstream of the 5' loxP sequence in pGKneoF2L2DTA. A 1.7-kb genomic sequence (3' targeting arm, short arm) downstream of *Adiponectin* exon 2, bounded by an EcoRV site, was cloned downstream of the 3' loxP sequence. A 3.5-kb region (conditional knockout region, knockout arm) was cloned between the 5' loxP sequence and the 5' FRT sequence. The resulting vector was verified by DNA sequencing and restriction mapping. The vector was linearized at the SacII site upstream of the 5' targeting arm and electroporated into 129SvEv-derived embryonic stem (ES) cells. Cells were then treated with G418, and negative selection was accomplished by the diphtheria toxin A cassette (DTA) in the pGKneoF2L2DTA vector. Genomic PCR analysis was performed by using primers located 5' outside the 5' targeting arm and within the neomycin resistance cassette and 3' of the 3' targeting arm and within the neomycin resistance cassette, respectively. PCR products were sequenced. More than 50 *Adiponectin* targeted ES clones were identified. Six of them were expanded and injected into C57BL/6 blastocysts that were transferred to the uterus of pseudo pregnant females. Floxed allele positive offspring were genotyped using PCR with the following primer sets: APN-floxed 5'- GGTGGCTCACAACCATTCATAA and 5'- CATACTCGCCTCTCCCAGAG.

Tissue and Serum Immunoblotting

For tissue immunoblotting, frozen tissues were homogenized in RIPA buffer (1% Triton-X100, 50 mmol/L Tris-HCl (pH 8.0), 0.25 mol/L NaCl, 5 mmol/L EDTA) containing protease inhibitor cocktail (#P8340; Sigma). The homogenates were centrifuged at 12,000g for 15 min at 4°C and the supernatants were assayed for protein content using a BCA assay kit (#23225; Thermo Fisher Scientific). Tissue protein (20 µg) or serum (0.1 µl) was separated by 4–12% sodium dodecyl sulfate-polyacrylamide gel (SDS-PAGE), transferred to nitrocellulose membranes (#162-0112; Bio-Rad), and blotted with anti-mouse adiponectin monoclonal (1:1000; produced in-house) [2]. The adiponectin antibody was validated using serum from a congenital APN knockout mouse as a negative control and serum from a wild type mouse as a positive control. Primary antibodies were detected using secondary antibodies labelled with infrared dyes emitting at 700 nm (1:5000; #926-32220; Li-Cor Bioscience; Lincoln, NE) or 800 nm (1:5000; #926-32211; Li-Cor Bioscience) and then visualized on a Li-Cor Odyssey infrared scanner (Li-Cor Bioscience). The scanned data were analysed and quantitated using Odyssey Version 2.1 software (Li-Cor Bioscience).

Systemic tests

For oral glucose tolerance tests (OGTTs), mice were fasted for 3 hours prior to administration of glucose (2.5 g/kg body-weight by gastric gavage; Sigma; St. Louis, MO). For insulin tolerance tests (ITTs), mice were fasted for 3 hours and then intraperitoneally injected with 0.75 U/kg body weight human insulin (Humulin R; Eli Lilly; Indianapolis, IN). For triglyceride clearance, mice were fasted overnight (~15 h), then orally gavaged with 15 µl/g body weight of 20% intralipid (#I141; Sigma). In the hepatic VLDL-TG production assay, mice were fasted for 5 hours, followed by intravenous

injection of 10% tyloxapol (T8761; Sigma) at 500 mg/kg body weight. At the indicated time-points, tail venous blood samples were collected in heparin-coated capillary tubes for OGTTs and ITTs and EDTA-coated capillary tubes for the triacylglycerol clearance and the hepatic VLDL-TG production assays. Glucose levels were measured using an oxidase-peroxidase assay (#P7119; Sigma), insulin levels were measured using commercial ELISA kits (#EZRMI-13K; Millipore; Billerica, MA), and triglycerides were measured using Infinity Triglycerides Reagent (#TR22421; Thermo Fisher Scientific; Waltham, MA).

Body Fat Quantification

Total body lean mass and fat was quantified using a Bruker MQ10 NMR analyser.

^{3}H-triolein uptake and β-oxidation

Measurements of endogenous triolein clearance rates, tissue-specific lipid uptake and β-oxidation rates in transgenic tissues were performed as previously described [3]. Briefly, ^{3}H-triolein (#NET431001MC; PerkinElmer; Waltham, MA) was tail-vein injected (2 μCi per mouse in 100 μl of 5% intralipid) into mice after a 5-hour fast. Tail blood samples (10 μl) were then collected at 1, 2, 5, 10, 15, and 20 min after injection. At 20 minutes following injection, mice were euthanized and tissues were quickly excised, weighed and frozen at −80 °C until processing. Lipids were then extracted using a chloroform-to-methanol based extraction method. The radioactivity content of tissues, including blood samples, was quantified as described previously [4].

Gene Expression Analysis

Tissues were excised and snap-frozen in liquid nitrogen. Total RNA was isolated following tissue homogenization in Trizol (Invitrogen; Carlsbad, CA) using a TissueLyser (MagNA Lyser; Roche; Indianapolis, IN), then isolated using an RNeasy RNA extraction

kit (#74104; Qiagen; Germantown, MD). cDNA was prepared by reverse transcribing 1 μg of RNA with an iScript cDNA Synthesis Kit (#1708891; Bio-Rad; Hercules, CA). **ESM Table 3** details the primer sequences that were utilized for quantitative RT-PCR. Quantitative PCR was performed using SYBR Select Master Mix (#4472908; Thermo Fisher; Waltham, MA). mRNA levels were calculated using the threshold cycle method [5], with Rps18 used for normalization.

iKO (n=3) and WT (n=3) littermate controls were fed a HFD for 4 weeks and then put on HFD-dox for adiponectin depletion for 2 weeks. Complete serum depletion of adiponectin was observed on 14 days post-dox treatment and tissues were collected from iKO and WT controls 3 days later. Global gene expression profiling by Affymetrix microarray analysis was conducted at the UTSW Genomics and Microarray Core. Total RNA samples from sWAT and Liver of iKO and WT mice were hybridized to GeneChip Mouse Transcriptome Assay v.1.0 (Affymetrix) according to the manufacturer's protocols. Normalization and statistical analysis were performed using Transcriptome Analysis Console v.3.0 (Affymetrix). Gene ontology analysis was performed using the NIH database DAVID Functional Annotation Tool (https://david.ncifcrf.gov/). Primary Component Analysis of both sWAT and Liver data was conducted in RStudio (v3.3). The heatmap was generated through RStudio (v3.3) using the Pheatmap package.

Streptozotocin (STZ) Administration and FGF21 stimulation of adipocytes.

Mice were fasted for six hours and subjected to a single intraperitoneal injection of streptozotocin (STZ; #S1030; Sigma) at the dose of 200 μg/g body weight. STZ was stored at -20°C as powder and freshly diluted in ice-cold sodium citrate buffer (0.1M, pH = 4.5) before injection. FGF21 (LY240,5319; Eli Lilly Inc.; Indianapolis, IN) was injected intraperitoneally at 2 mg/kg body weight.

Computed Tomography

Mice were anesthetized with isoflurane and a CT scan was performed at a resolution of 93μm using short scan mode (180°) on an eXplore Locus *in vivo* MicroCT scanner from GE Healthcare (Little Chalfont, Buckinghamshire, UK) as previously described [6].

Immunohistochemistry

For F4/80 immunohistochemistry, paraffin-embedded sections were incubated with anti F4/80 (1:500; MCA497; Bio-Rad), followed by secondary and tertiary signal amplification and detection using biotinylated anti-rat secondary (#BA-9400; Vector; Burlingame, CA), HRP-conjugated streptavidin (#P0307; Dako; Santa Clara, CA), and DAB substrate (#34002; Thermo Fisher Scientific; Waltham, MA).

In situ hybridization

RNAscope 2.5 HD Assay-Brown (Bio-Techne; Minneapolis, MN), a novel in situ hybridization (ISH) technique designed to visualize cellular RNA targets in tissues fixed in 10% formalin [7], was used for detecting adiponectin RNA in adipose tissue of mice treated with HFD containing pioglitazone (40 mg/kg provided as an add-mix in Bio-Serve S5867). The cRNA probe for adiponectin was generated by RNAscope. Hybridizations were performed according to the manufacturer's instructions.

Lipoprotein lipase activity assay

Lipase activity was measured as previously described [8] with minor modifications. Briefly, pre- and post-heparin plasma was collected from mice before and after 15 min after tail vein injection of heparin (1.5 U/g BDW, #H3393; Sigma; St. Louis, MO), respectively. Per 0.2 ml reaction, 10 µl of plasma was incubated with a triacylglycerol emulsion containing ~10^7 cpm/ml ^{3}H-triolein (#NET431001MC; PerkinElmer; Waltham,

MA) at 37°C water bath for 90 min for total lipase activity, or with 1.5 M NaCl for hepatic lipase activity. Reaction was terminated by addition of 3.25 ml methanol:chloroform:heptane (1.41:1.25:1) and 1.05 ml K_2CO_3 (pH 10.5). After vigorous agitation and centrifugation, 1 ml of the NEFA-containing aqueous phase was transferred and assayed for ^3H radioactivity on a scintillation counter. Serial dilutions of a lipoprotein lipase (0, 10, 20, 50, and 100 ng, #L9656; Sigma; St. Louis, MO) were parallel assayed as standard controls, and the lipase activities of plasma samples were calculated as equivalents of the standard lipase. The plasma lipoprotein lipase activity was calculated by subtracting the hepatic lipase activity from the total.

Lipid quantifications

Sphingolipids were quantified as described previously by liquid chromatography-electrospray ionization-tandem mass spectrometry (LC/ESI/MS/MS) using a Shimadzu Nexera X2 UHPLC system coupled to a Shimadzu LCMS-8050 triple quadrupole mass spectrometer [9]. Mass spectrometry data was processed using Lab Solutions and Lab Solutions Insight packages of programs.

Diacylglycerol and C17 FFA were quantified using an ABI 5600+ (AB Sciex) following direct infusion of extracted lipids containing 18 mM ammonium fluoride to aid in ionization of neutrals and to reduce salt adducts. Data from the AB Sciex 5600+ was collected and calibrated with Analyst and PeakView Software (AB Sciex) [9]. Lipid species were identified based on exact mass and fragmentation patterns and verified by lipid standards.

Supplemental References

[1] Hoch RV, Soriano P (2006) Context-specific requirements for Fgfr1 signaling through Frs2 and Frs3 during mouse development. Development 133: 663-673

[2] Schraw T, Wang ZV, Halberg N, Hawkins M, Scherer PE (2008) Plasma adiponectin complexes have distinct biochemical characteristics. Endocrinology 149: 2270-2282

[3] Wada I, Rindress D, Cameron PH, et al. (1991) SSR alpha and associated calnexin are major calcium binding proteins of the endoplasmic reticulum membrane. J Biol Chem 266: 19599-19610

[4] Kusminski CM, Holland WL, Sun K, et al. (2012) MitoNEET-driven alterations in adipocyte mitochondrial activity reveal a crucial adaptive process that preserves insulin sensitivity in obesity. Nat Med 18: 1539-1549

[5] Livak KJ, Schmittgen TD (2001) Analysis of relative gene expression data using real-time quantitative PCR and the 2(-Delta Delta C(T)) Method. Methods 25: 402-408

[6] Asterholm IW, Scherer PE (2010) Enhanced metabolic flexibility associated with elevated adiponectin levels. Am J Pathol 176: 1364-1376

[7] Xu Y, Wu Z, Sun H, et al. (2013) Glutamate mediates the function of melanocortin receptor 4 on Sim1 neurons in body weight regulation. Cell Metab 18: 860-870

[8] Razani B, Combs TP, Wang XB, et al. (2002) Caveolin-1-deficient mice are lean, resistant to diet-induced obesity, and show hypertriglyceridemia with adipocyte abnormalities. J Biol Chem 277: 8635-8647

[9] Holland WL, Miller RA, Wang ZV, et al. (2011) Receptor-mediated activation of ceramidase activity initiates the pleiotropic actions of adiponectin. Nat Med 17: 55-63

ESM Table 1

Gene	Forward 5'-3'	Reverse 5'-3'
Adipoq	AGATGGCACTCCTGGAGAGAA	TTCTCCAGGCTCTCCTTTCCT
Adipsin	CTACATGGCTTCCGTGCAAGT	AGTCGTCATCCGTCACTCCAT
Cebpα	CAAGAACAGCAACGAGTACCG	GTCACTGGTCAACTCCAGCAC
Fabp4	GATGAAATCACCGCAGACGAC	ATTCCACCACCAGCTTGTCAC
Lpl	CATCGAGAGGATCCGAGTGAA	TGCTGAGTCCTTTCCCTTCTG
Pparγ2	GCATGGTGCCTTCGCTGA	TGGCATCTCTGTGTCAACCATG
Lck	GGAGAAGGTCTGCGATTGATG	TTGAGCTCCTGGTGTGTGCTA
Lsp1	CCGATAGCCTCTCCTTTTGCT	ATCCTTCCTTGGGAGCTCTTG
Col1α1	AGATGATGGGGAAGCTGGCAA	AAGCCTCGGTGTCCCTTCATT
Col3α1	ATTCTGCCACCCCGAACTCAA	ACAGTCATGGGGCTGGCATTT
CD6	TCCTGTCCCTATCACCATTGC	TCCTGTCCCTATCACCATTGC
CD27	AGGTCGGTTTACCACCCAAGT	CTGCCCAGGGAGATCTTTTCT
CD52	TGCTACAGAGCCCAGGAAGAT	TTAGTACCAGAAGCGGCCGTA
CD79A	TGGGACCAGACAGTTCTTGCT	CTTGCTTTGGGACATGAGGAG
Ccl19	GTGAAAGCCTTCCGCTACCTT	TGGAGGTGCACAGAGCTGATA
Rps18	CATGCAAACCCACGACAGTA	CCTCACGCAGCTTGTTGTCTA

ESM Table 2

Experimental Cohorts			
HFD apnfl	Weight	SEM	
iKO	53.5	0.93	n=6
WT	56.5	1.88	n=7
Chow apnfl			
iKO	24.6	1.16	n=6
WT	26.4	1.35	n=8
STZ Treatment			
iKO	26. 8	0.84	n=6
APN KO	25.5	0.44	n=8
WT	27.6	0.60	n=8

ESM Table 3

Gene ID	P-value	Fold Change over WT
B630019A10RIK	0.022216537	10.33662699
ACDC	0.002215229	0.177462163
LOC620807	0.002911483	0.311455338
MUP2	0.001395558	0.318277899
MUP1	0.002402936	0.322959613
MUP2	0.007010177	0.341740417
MUP1	0.002895585	0.361325793
TRIM30	0.011611007	2.642843457
IGH-VJ558	0.031613294	2.407689267
IGH-VJ558	0.026182129	2.248957812
CD52	0.026210777	2.244941427
CCL5	0.004054771	2.233756615
LCK	0.00086422	2.22438487
C920004C08RIK	0.03662874	2.202779298
S100A9	0.022099788	2.178139341
CCL21B	0.004080561	2.156769012
CCL19	0.00565152	2.133379888
BCL11B	0.024467442	2.063903282
CCL19	0.00084539	2.0398309
OTTMUSG00000007485	0.001742138	0.491645861
2210421G13RIK	0.000978372	2.027596899
CCL21C	0.014175304	2.008296336
CCL21A	0.004558562	2.004930375
CD8B	0.003391395	2.00438417
CD3D	0.001871475	2.002639072
H2-M2	0.001018709	1.966372148
CD3G	0.003777068	1.961705126
NUP210	0.008613711	1.960074714
CCL21C	0.018058899	1.928992999
CD6	0.001870023	1.915519766
ST6GAL1	7.67468E-05	1.909988371
CD27	0.002474828	1.898866656
CD79B	0.018540288	1.895209215
ARL4C	0.022332683	1.89455805
NUDT6	0.002123248	0.531830742
CD3E	0.001939767	1.866984127

CD3E	0.000355908	1.856786427
LOC382896	0.001254658	1.852618477
ITK	0.001051039	1.851987142
SELL	0.004323084	1.850406548
9830148G24RIK	0.043125582	1.849444401
IL4I1	0.001780141	1.849418712
RGS10	0.010313011	1.838528523
TCRB-V8.2	0.002049688	1.830961913
RASGRP1	0.0007753	1.830857207
A130092J06RIK	0.000970897	1.829919258
CORO1A	0.002510863	1.828522715
TST	0.003302758	0.548300342
CYP2E1	0.017042459	0.549052226
1200013B08RIK	0.004750795	1.793376558
E430021P16RIK	0.002818651	1.790662074
9130430L19RIK	0.002829152	1.783039521
5830496L11RIK	0.011432124	1.781859756
CD79A	0.030457677	1.780181672
CD52	0.004497156	1.779472618
RASSF5	0.002328991	1.777167947
1810062O14RIK	0.011961958	1.776621933
SATB1	0.025801868	1.774800336
CTSW	0.006257894	1.770187913
A130065C13RIK	0.008265468	1.75826535
SAMSN1	0.000694544	1.758216222
CD6	0.000628203	1.753944885
LSP1	0.001229754	1.751951003
CLU	0.000220089	1.746220174
ZAP70	0.00263848	1.745539697
FSCN1	0.003002878	1.743644689
HP	0.029320526	0.574092519
2310046K10RIK	0.01001536	1.739651
6330406L22RIK	0.002168566	1.735227678
TCRB-V13	0.002033472	1.733732397
ITGB7	0.001672375	1.73111685
CORO1A	0.006290486	1.729332817
PSCDBP	0.004590354	1.72876429
KLRD1	0.007234915	1.722504371
IFITM1	0.000737722	1.719847085

SERPINA3G	0.001386671	1.714165604
ITGAE	0.04035548	1.713064871
A430107D22RIK	0.011015394	1.709157175
1810037B05RIK	0.008157189	1.708180256
IGH-6	0.033086605	1.705966074
FCRLA	0.029168257	1.702533054
MELA	0.01041098	1.701421283
NNMT	0.037777257	0.588524857
PDE4B	0.003460231	1.69412
6330500D04RIK	0.006213951	1.692303427
FCRLA	0.013862212	1.688883881
KLHL6	0.010911127	1.687677054
D230007K08RIK	0.010491927	1.685708248
BACH2	0.011710528	1.684292178
LAT	0.020164719	1.679341196
TCF7	0.005013593	1.668710152
LBH	0.010872434	1.668133696
LBH	0.016674208	1.66579537
BCL11A	0.016203938	1.665209013
KLHL6	0.006249129	1.662409701
ARHGAP30	0.00349934	1.662310649
AI467606	0.001951922	1.660947516
CD53	0.008318141	1.659533621
SPATA13	0.007466505	1.657919266
SH3BGRL3	0.004585865	1.65770945
CD2	0.00514902	1.657679596
SELPL	0.010953988	1.655656925
PRKCB	0.014486398	1.655023923
BC064033	0.017376079	1.648763064
A130090K04RIK	0.011496578	1.647283491
ARHGDIB	0.002903961	1.646628327
5830472H07RIK	0.005531759	1.645966146
FYB	0.004523662	1.645825366
0610039P13RIK	0.015396189	1.644246431
IGLC2_J00595_IG_LAMBDA_CONSTANT_2_14	0.037677273	1.643935799
ZFPN1A1	0.004151279	1.639417894
SERPINA3C	0.000615953	0.610247052
SLC27A1	0.031888032	0.610321311
ARHGEF1	0.004178748	1.636441754

GALGT1	0.007982847	1.632900177
A630006E02RIK	0.006851765	1.631542857
B830021E24RIK	0.02393371	1.628461242
RAC2	0.020994546	1.6243973
HCST	0.007607879	1.623048164
NKG7	0.001846899	1.622889034
HP	0.044403939	0.616613058
GPR83	0.01247885	1.620711167
TRIM34	0.014513612	1.620164756
CORO1A	0.002728111	1.619007269
ITGAE	0.032075751	1.618601986
CD28	0.000952481	1.615514334
ARHGAP4	0.006933322	1.611702479
HCPH	0.006465156	1.609389937
HP	0.021773648	0.622040282
2310046K10RIK	0.023968889	1.60626732
2210408F11RIK	0.000727618	1.605212135
CD6	0.004497693	1.603494624
DGKA	0.020549745	1.597711575
IL7R	0.008810159	1.597180574
CXCL16	0.003500362	1.596302631
SH2D2A	0.002422003	1.596242424
GPR18	0.018315856	1.596035061
TRIM34	0.014209928	1.594712915
BTG1	0.004118957	1.592208756
EGR3	0.002581592	1.592191379
6330500D04RIK	0.012091199	1.590943396
MALT-1	0.018858019	1.587524831
CENTB1	0.01455859	1.587272569
LOC193676	0.001100528	1.586167616
FBN1	0.024828223	0.630556606
COTL1	0.000354858	1.585294345
LTB	0.023814809	1.58517419
TSPAN32	0.021198268	1.583731682
VCAM1	0.014691673	1.58359616

ESM Figure 1

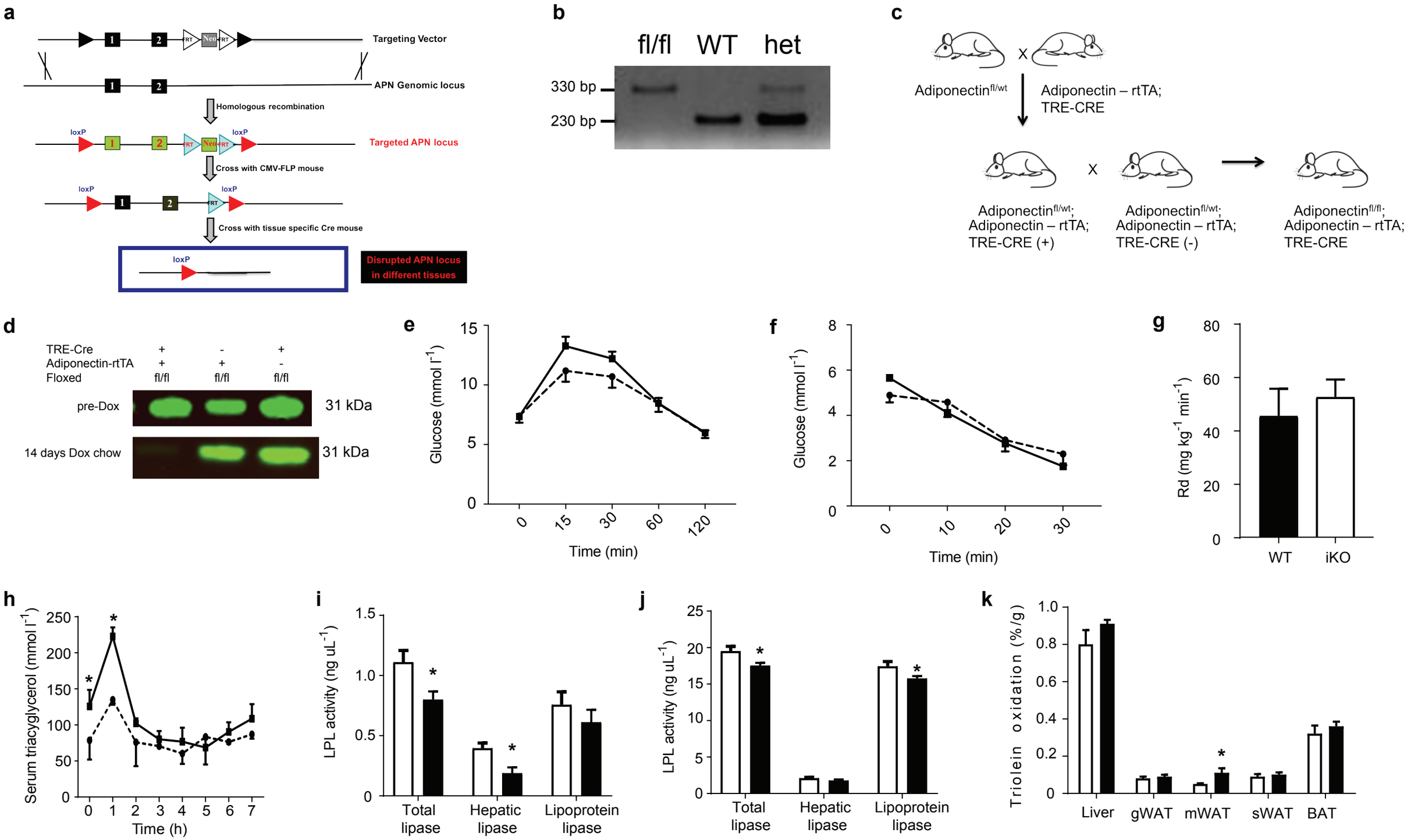

ESM Fig. 1. Generation of iKO mice and subsequent metabolic phenotyping **a)** A schematic of flanking the first 2 adiponectin exons with loxP sites for the generation of the conditional knockout mouse. **b)** Agarose gel electrophoresis shows pups that are fl/fl (330bp), WT (230 bp), and heterozygous (both 330 bp and 230 bp). **c)** Planned breeding of adiponectin $^{fl/fl}$ mice to adiponectin-rtTA and TRE-Cre for the synthesis of the iKO mouse. **d)** Representative immunoblots of serum adiponectin of male adiponectin fl/fl mice and WT littermate controls after 14 days of chow-dox diet. **e)** Circulating glucose levels were measured in iKO (solid line, n=5) and WT (dashed line, n=6) littermates during an oral glucose tolerance test (OGTT) (2.5g/kg glucose per oral gavage) after 14 days of chow-dox diet. **f)** Circulating glucose levels were measured in iKO (solid line, n=5) and WT littermates (dashed line, n=6) during an Insulin Tolerance Test (ITT) (0.75U/kg insulin per IP injection) after 14 days of chow-dox diet. **g)** Rate of glucose disappearance for WT and iKO mice during hyper-insulinemic euglycaemic clamp after 6 weeks of HFD feeding followed by 2 weeks of HFD-dox. **h)** Circulating triglyceride (TG) levels were measured during an oral TG clearance test (20% intralipid, 15 uL/g body weight; single gavage) in iKO (solid line, n=6) mice and WT (dashed line, n=8) littermate controls after 2 weeks of chow-dox diet. **i)** Preheparin lipoprotein lipase activity levels of iKO (black bars, n=6) and WT (white bars, n=8) mice after 2 weeks of chow-dox diet. **j)** Post-heparin lipoprotein lipase activity levels of iKO (black bars, n=6) and WT (white bars, n=8) mice after 2 weeks of chow-dox diet. **k)** Total ^{3}H-triolein lipid-oxidation per tissue in male iKO (black bars, n=6) and WT (white bars, n=6) mice at 15 min after injection (2 µCi per mouse in 100 µl of 5% intralipid, single tail-vein injection) after 4 weeks of HFD-dox. * denotes $p<0.05$ by Students T-test

ESM Figure 2

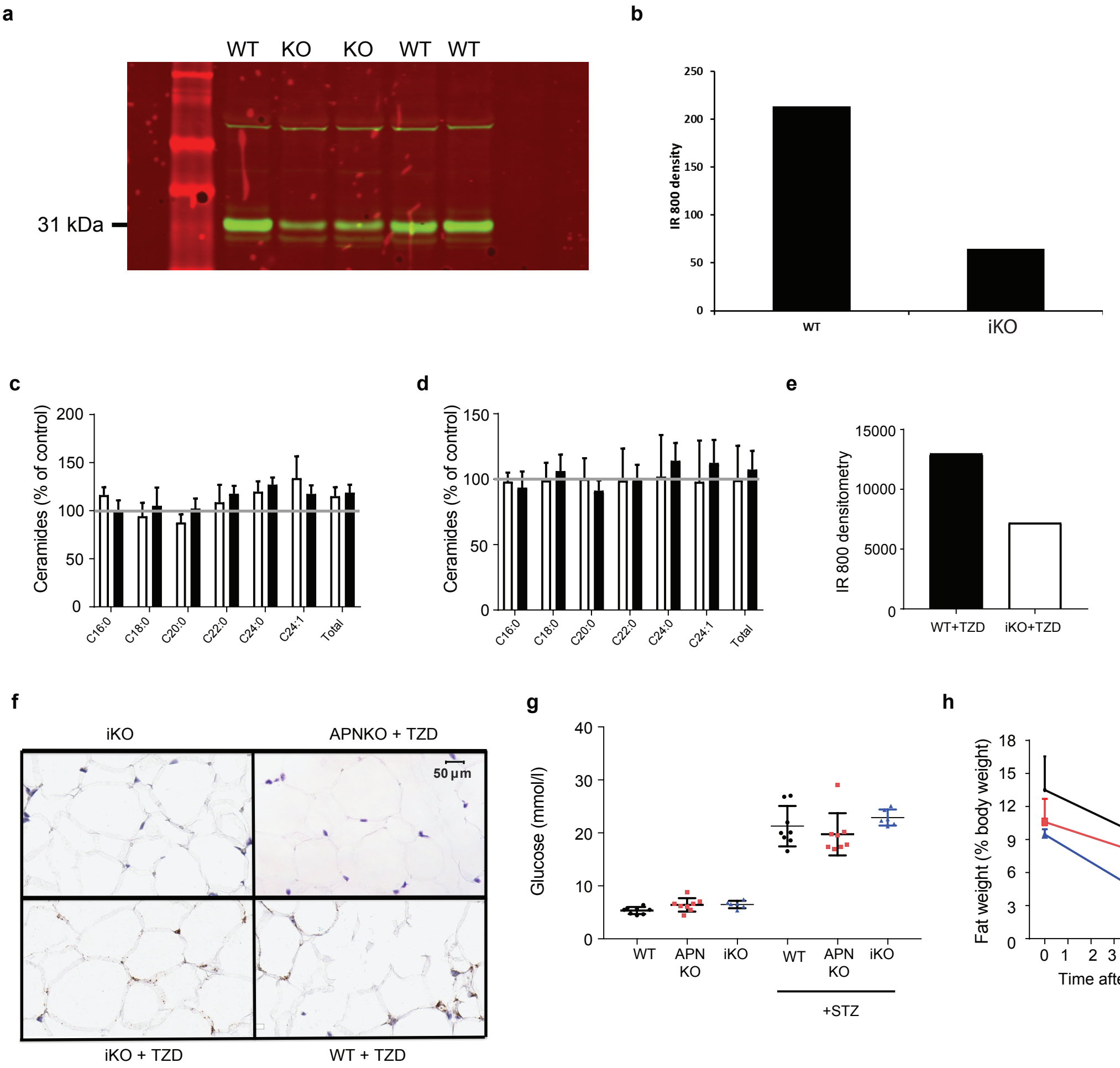

ESM Fig 2. FGF21 and TZDs can induce increase in serum adiponectin post-Inducible adipose-specific deletion of adiponectin.

a) Representative immunoblot of SWAT adiponectin levels in adiponectin floxed mice and WT controls after 2 weeks of chow-dox feeding. **b)** Quantification of immunoblot bands of SWAT adiponectin levels in adiponectin floxed mice and WT controls from ESM Fig. 2a. **c)** Analysis of liver ceramide species from APNKO mice (white bars, n=7) and APNKO mice (black bars, n=8) 1 day after of intraperitoneal injection of FGF21 (2mg/kg) in mice fed chow-dox for 2 weeks. **d)** Analysis of subcutaneous adipose tissue (SWAT) ceramide species from APNKO mice (white bars, n=7) and APNKO (black bars, n=8) 1 day after intraperitoneal injection of FGF21 (2mg/kg) in mice fed chow-dox for 2 weeks. **e)** Quantification of immunoblot bands of serum adiponectin levels in iKO and WT controls at day 60 of time course of HFD supplemented with pioglitazone after 2 weeks chow-dox feeding. **f)** In Situ hybridization to adiponectin RNA at day 60 of time course of HFD supplemented with pioglitazone after 2 weeks chow-dox feeding. **g)** Serum glucose levels in iKO (n=6), APNKO (n=8) and WT (n=8) mice pre and post-STZ injection after 2 weeks dox-chow diet. **h)** Weight loss of iKO (blue line), APNKO (red line), and WT (black line) controls after injection of STZ.

ESM Figure 3

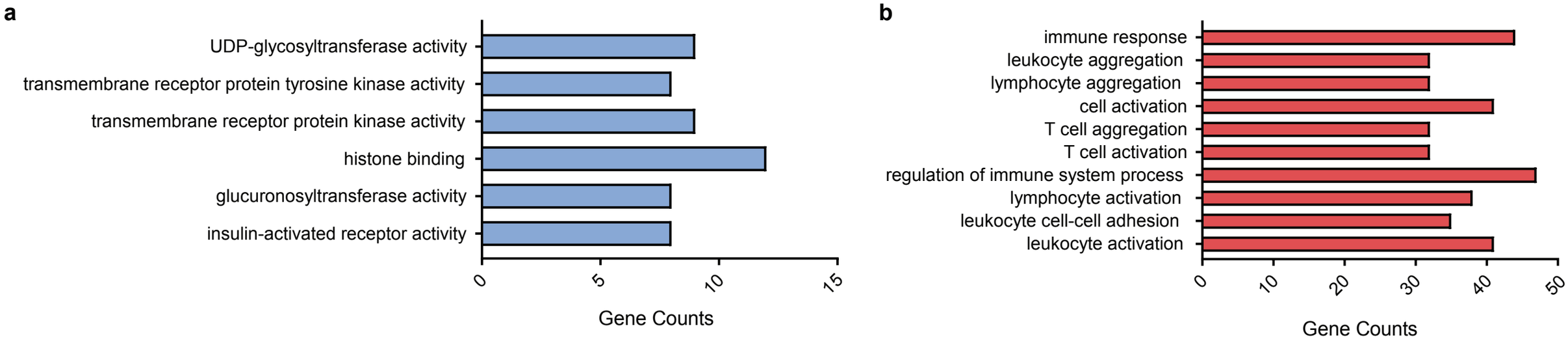

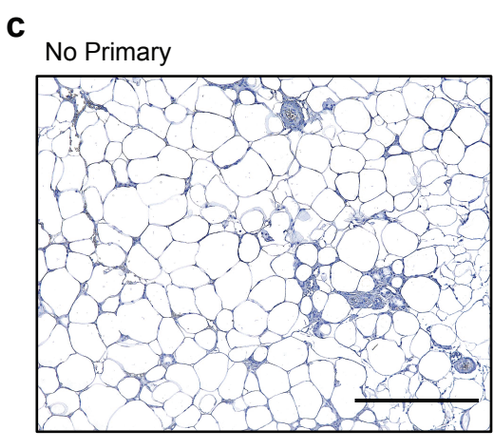

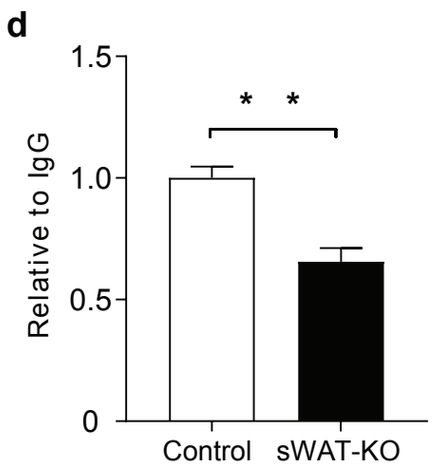

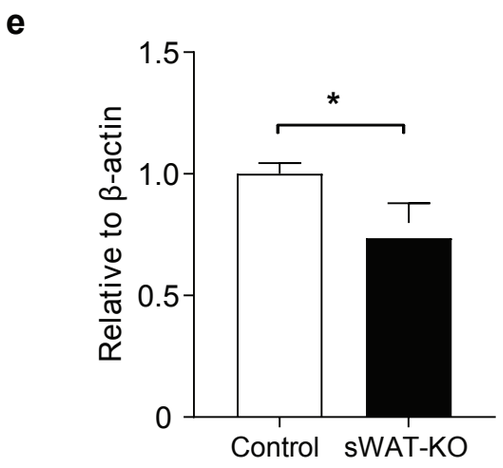

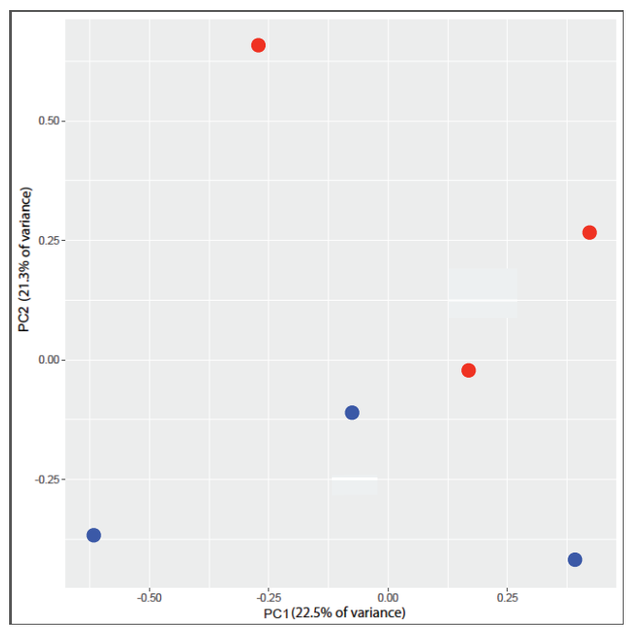

ESM Fig. 3 Microarray of subcutaneous adipose tissue of adipose-specific deletion of adiponectin mice and WT controls show significant upregulation of inflammatory genes in iKO mice.

a) Gene ontology analysis showing number of statistically significant downregulated SWAT genes of iKO mice with at least 2 fold change over WT controls after 4 weeks of HFD feeding followed by 2 weeks of HFD-dox . **b)** Gene ontology analysis showing number of statistically significant upregulated SWAT genes of iKO mice with at least 2 fold change over WT controls after 4 weeks of HFD feeding followed by 2 weeks of HFD-dox. **c)** Representative F4/80 stained images of iKO SWAT without primary antibody added (scale bar = 400 μm) after 4 weeks of HFD feeding followed by 2 weeks of HFD-dox. **d)** Quantification ratio of adiponectin to IgG in the serum adiponectin immunoblot done on LICOR Odyssey Scanner in WT (n=3) and SWAT-KO (n=3) mice at 1 month of age. **e)** Quantification ratio of adiponectin to β-actin in subcutaneous adiponectin immunoblot done on LICOR Odyssey Scanner in WT (n=3) and SWAT-KO (n=3) mice at 1 month of age. **f)** Principle component analysis performed on the significantly changed Liver genes of iKO (red) and WT (blue) controls (n=3) after 4 weeks of HFD feeding followed by 2 weeks of HFD-dox. * denotes $p<0.05$, **$p<0.01$ by Students T-test